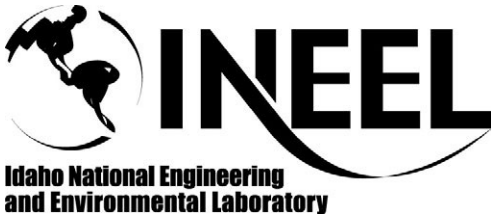

INEEL/CON-00-01663
PREPRINT

Ultrasonic Imaging of Subsurface Objects Using Photorefractive Dynamic Holography

Vance A. Deason
Kenneth L. Telschow
Scott Watson

July 29, 2001

SPIE 46th Annual Meeting on Optical Science and Technology

Ultrasonic Imaging of Subsurface Objects Using Photorefractive Dynamic Holography

Vance A. Deason, Kenneth L. Telschow, Scott Watson
Idaho National Engineering and Environmental Laboratory
PO Box 1625, MS 2211, Idaho Falls ID, 83415

ABSTRACT

The INEEL has developed a photorefractive ultrasonic imaging technology that records both phase and amplitude of ultrasonic waves on the surface of solids. Phase locked dynamic holography provides full field images of these waves scattered from subsurface defects in solids, and these data are compared with theoretical predictions. Laser light reflected by a vibrating surface is imaged into a photorefractive material where it is mixed in a heterodyne technique with a reference wave. This demodulates the data and provides an image of the ultrasonic waves in either 2 wave or 4 wave mixing mode. These data images are recorded at video frame rates and show phase locked traveling or resonant acoustic waves. This technique can be used over a broad range of ultrasonic frequencies. Acoustic frequencies from 2 kHz to 10 MHz have been imaged, and a point measuring (non-imaging) version of the system has measured picometer amplitudes at 1 GHz.

Keywords: interferometry, laser ultrasound, dynamic holography, ultrasonic imaging, photorefractivity

1. INTRODUCTION

Ultrasonic inspection techniques have become a mainstay of the nondestructive testing (NDT) community. Ultrasonic waves penetrate optically opaque materials and interact with hidden flaws, microstructural features and sample geometry to reveal information about the nature and severity of these flaws and features. While contacting piezoelectric excitation and detection methods are highly developed and well understood, they are generally limited to detection at a single point and transducers must normally be in contact with the object. Arrays of contacting transducers can be used to make area maps of acoustic distributions, and phased arrays of transducers can be used to sweep out and image extended volumes.

In recent years, many researchers have worked to develop noncontacting optical excitation and detection methods for making ultrasonic measurements using pulsed and continuous wave (CW) lasers [1,2,3]. Excitation usually involves generation of acoustic waves though thermal expansion or ablative processes at the material surface induced by tightly focussed laser pulses. These processes typically generate broadband acoustic waves whose frequency content is determined by laser pulse duration, spot size and thermal relaxation processes in the material. Detection involves interferometry using CW lasers, and can be implemented in a variety of ways ranging from simple Michelson interferometers to more recent systems incorporating nonlinear photorefractive detection schemes. Laser ultrasonic techniques have many applications in research and NDT, and several companies now offer commercial systems for this type of measurement.

Like contacting piezoelectric transducers, the laser ultrasonic process is normally a point measurement technique, although systems are available for scanning the laser spot over an extended area to build up an image of the acoustic motion distribution across the surface. At the INEEL, we have developed an alternative technique that inherently produces images of the distribution of acoustic waves over an extended surface, and does so at video frame rates (~30 frames/second). Spatial resolution is high, since we can take advantage of modern CCD array detectors, where each pixel becomes an amplitude and phase detector. Currently we use 12 bit, 1000x1000 pixel array cameras with full field frame rates of 15 frames/sec (fps) and 2x2 binned image rates of 15 fps. This essentially places 10^6 measurement points across the surface 15 times per second. With the current system, we can detect acoustic displacement amplitudes of about 1 to 10 nanometers, with a noise floor of about 0.1 nm. A related system configured as a single point detector is capable of resolving acoustic wave displacement amplitudes on the picometer scale [4]. In all cases, full control of acoustic phase is available, to provide either static, fixed phase images or phase stepped video animations of the wave motion.

2. THE INEEL LASER ULTRASONIC CAMERA

The INEEL Laser Ultrasonic Camera consists of a diode pumped, solid state laser, EO modulator (EOM), photorefractive demodulator and a CCD camera. A computer is used to acquire, store, manipulate and display the images. Figure 1 shows the

general layout of the system, which can be configured for a variety of applications, including macroscopic or microscope subjects, specular or diffuse objects, using 2 wave or 4 wave mixing modes, etc.

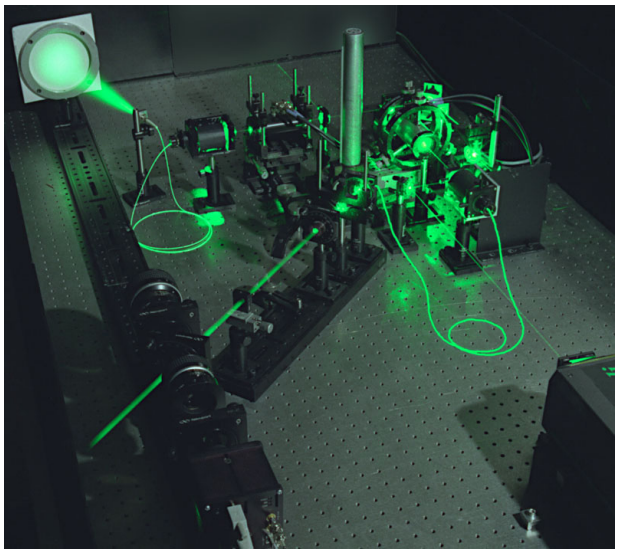

(a)

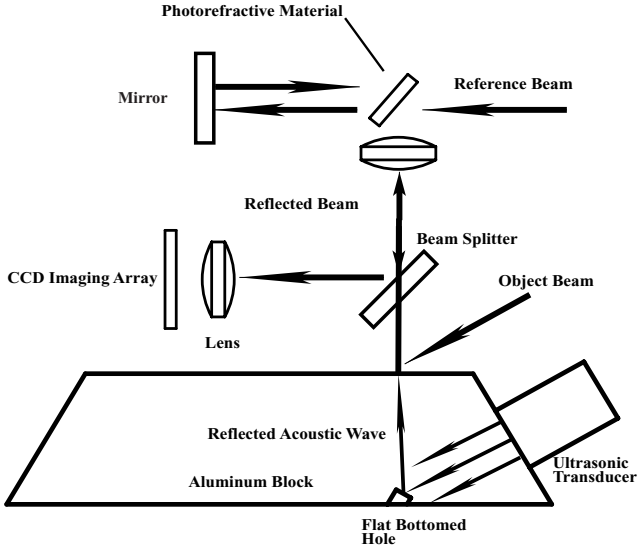

(b)

Figure 1: (a) Optical set-up for the laser ultrasonic camera (b) Sample measurement geometry

3. EXPERIMENTAL CONFIGURATIONS

A Coherent 5-Watt (1 to 2 watts used, depending on surface reflectance of subject) Verdi™ laser is used to illuminate the vibrating object and to provide a reference beam for interferometric measurement of the vibration amplitude. The object wave reflects from the surface of the specimen and is imaged into the photorefractive plate of Bismuth Silicon Oxide (BSO) to form a phase grating. This grating is moving due to a small offset between the specimen and EOM frequencies. The BSO plate is 2.25 mm thick and 20x20 mm square. Interferometry is performed in the plate by mixing a reference beam with the object beam to form the phase grating or dynamic hologram. The reference beam simultaneously reconstructs this hologram. While the system can be operated in either 2-wave or 4-wave mixing modes, this report describes data taken in 4-wave mode. Figure 1a shows the system in 2-wave mixing mode, measuring ultrasonic vibrations traveling in copy paper. As shown in Figure 1b, the 4-wave mode involves reflecting the reference beam back through the photorefractive crystal so as to diffract a phase conjugate beam toward the object. A partially reflecting mirror picks off this beam and directs it to the camera, where it is recorded and digitized. As is explained elsewhere [4], the intensity of this image is proportional to the amplitude of the vibration.

This report focuses on imaging bulk acoustic waves at the sample surface after having been reflected from buried scatterers and geometrical surfaces. The surfaces of these samples were polished to enhance optical reflectivity, although the technique easily handles diffusely reflecting surfaces due to its holographic nature. Measurements were made in 4-wave mode and typical acoustic displacement amplitudes were on the order of a few nanometers at a frequency of 9.3 MHz.

Specimens: several thick aluminum specimens were fabricated, some with flat-bottomed holes drilled in various patterns. A typical specimen is shown in Figure 2. An ultrasonic transducer was used to insonify the sample, directing an acoustic beam at a particular face of the sample, so as to pass through or reflect from an internal feature or defect. In the latter case, the reflected acoustic beam was measured at the top surface of the sample, where the spatial distribution of amplitude and phase of the acoustic wave normal displacement was recorded. For each defect type (including a defect free zone), a record was made of surface displacements due to the transmitted and reflected waves, as well as images of the surface without insonification. A test target for magnification scaling was also imaged. In some cases, a longer series of images was recorded where the relative phase of the acoustic wave was advanced by 10 degrees per step, in order to construct an animation of the acoustic wave front over a full 360 degrees of phase variation. Such movies are often quite revealing, and demonstrate the power and utility of the INEEL Laser Ultrasonic Camera. Because the process is essentially a CW (continuous acoustic wave) detection scheme, some effort was given to reduce stray reflections of acoustic energy. This was done by covering key

areas of the sample surface with thin sheets of Sorbothane™ absorbent material [5], leaving uncovered only those regions needed for mounting, viewing and insonification.

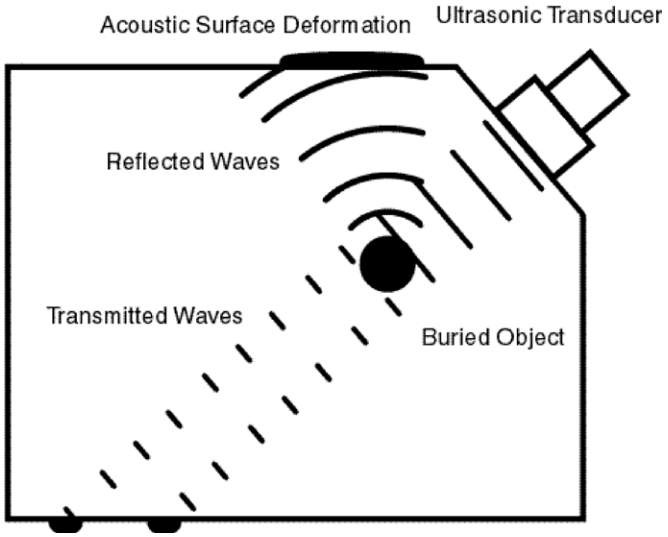

Figure 2: acoustic scattering patterns from buried objects and location of imaging (transmitted and reflected) measurement surfaces

4. DATA ACQUISITION AND ELECTRONICS

The INEEL Laser Ultrasonic Camera has a nominal detection range for acoustic amplitude of 40 nm to 0.1 nm and is basically operable at any acoustic frequency. The present imaging system is limited by electronics to about 12 MHz. Amplitudes above 45.7 nm, corresponding to the first peak of the Bessel response function product, can be recorded, but are ambiguous due to the multi-valued response curve. However, such features as nodes are clearly delineated. Below 10 nm or so, the response is nearly linear. Below ~0.1 nm, phase noise dominates for the present imaging system. We have demonstrated single point measurements, based on the same technology, with picometer resolution out to 1 GHz [6]. In order to improve the signal to noise ratios and the visual appearance of the data, each image shown here and each frame of a corresponding movie was averaged 32 times. Images are collected by a SMD/Dalsa 1M-15 12 bit, 1 mega-pixel grayscale camera. This camera is normally run in 512x512 2X binning mode at <30 frames per second. Images and sequences of images are acquired by the proprietary SMD software and saved to disc under the Windows NT™ operating system. A second computer running Windows 98™ controls all other aspects of the experiment through custom LabView™ drivers. Four function generators (1 ea. HP3312A and 3 ea. Stanford DS345) control timing and phase and provide a phase locked synthetic difference frequency for calibration purposes. Two ENI 2100L RF amplifiers power the New Focus 4002 optical phase modulator and the ultrasonic transducer used to insonify the target. Various waveplates, beamsplitters, lenses and mirrors control laser beam shape, orientation and polarization.

The reference beam is modulated at a frequency differing from the acoustic frequency by a small amount, ΔF (usually a few Hertz). This generates a moving grating in the photorefractive crystal. Details of this process and a full description of the theoretical basis of the Camera are available in [4, 7]. Data are acquired at 0 and 180 degrees phase in ΔF and subtracted to form a single movie frame or still image. This is done to remove a large constant or DC component of the image intensity. For averaging, 32 such frames are created and averaged to form a single final image. All of the data presented in this report was collected using the 4-wave mixing mode, where the data image is counter-propagated (phase reversal) back along the object beam and picked off and sent to the camera by a partially reflecting mirror. This mode provides the cleanest data for specular reflecting objects. The 2-wave mixing mode works well for diffusely reflecting objects.

Calibration data: The imaging measurements were calibrated as to the acoustic displacement by recording a set of images where the relative dynamic phase difference between the object and reference beams was synthetically varied between 0 degrees and an amount somewhat greater than that corresponding to about 45 nm of actual displacement. This traces out the image intensity curve corresponding to the theoretically predicted response function, a product of Bessel functions $\{J_0 * J_1\}$ of

the dynamic phase amplitude. The peak of this curve corresponds to 45.7 for the 532 nm laser wavelength used. Figure 3 shows a typical calibration curve where the raw data (in camera "counts") is plotted versus the modulation voltage (this voltage is further amplified before it is applied to the EO phase modulator). A least squares fit to the Bessel function product is made, and the resulting curve plotted along with the raw data. In the lower range (<1 volt or 10 nm) the curve is very nearly linear. This calibration can be used to transform an image in intensity units to a corresponding image in acoustic displacement units (nm) with a color bar scale.

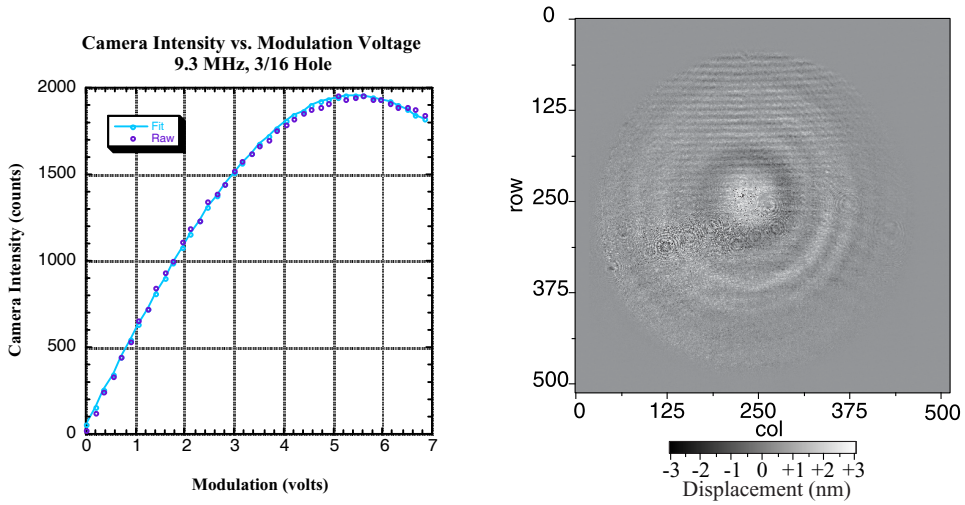

Figure 3: Calibration curve taken for the 3/16 inch hole data and the corresponding gray scale calibration for acoustic displacement

5. RESULTS

Graduated hole pattern: this consists of 3 flat bottomed holes with diameters of 1/8, 3/16 and 1/4 inch, plus a region free of holes to serve as a reference. Each hole was insonified by a 3/4 inch wafer transducer at 9.3 MHz, and was oriented so as to reflect ultrasonic waves from the transducer to a specified region on the top surface of the block. Data were taken on both the top (reflected wave) and bottom (transmitted wave) surfaces of the block. As indicated earlier, the transmitted wave was seen on the surface from which the hole was drilled and is partially blocked by the hole. An example of the image data for the 3/16 inch hole is shown in Figure 4.

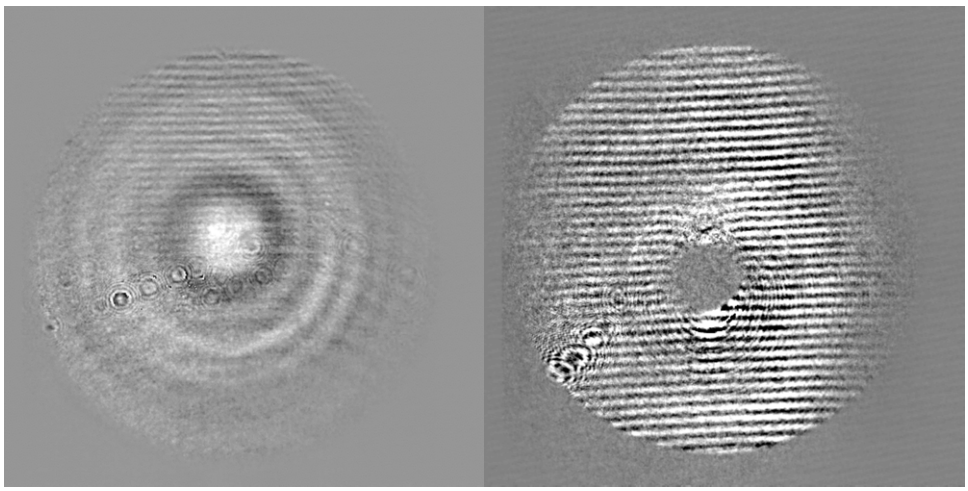

Figure 4: Reflected (left) and transmitted (right) acoustic displacement images for the 3/16 inch diameter flat bottomed hole at 9.3 MHz.

For each of these holes, the data clearly show the effect of the hole's presence on both the reflected and transmitted waves. The transmitted wave image is taken in the acoustic near-field of the transducer, resulting in rather complex scattered wavefront images. The transmitted wave images show acoustic plane wavefronts reflecting off the sample surface oriented at and approximate angle of 30 degrees with respect to the transducer normal. Shadowed waves are also present due to blockage and diffraction by the hole (Figures 4-right and 5-right). In contrast, the images recorded at the reflected wave sample surface (Figure 4) show diffraction from the flat bottom hole much like that from an equivalent circular piston transducer operating in the acoustic far-field. These results are consistent with our acoustic understanding of the scattering occurring off a flat bottomed hole buried within the object. Efforts are underway to develop a tone burst mode of operation to help eliminate interference due to multiple acoustic reflections within the sample.

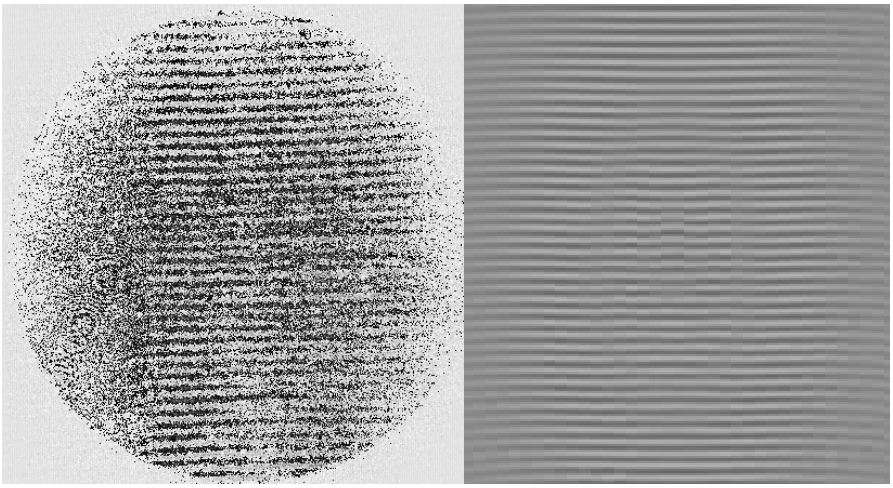

Figure 5: Comparison images of measured (left) and computed (right) acoustic wave displacements for the transmitted no-flaw case

Figure 5 shows a recorded wavefront from direct specular acoustic reflection off the transmitted sample surface made in the absence of a flaw and a computed wavefront for the same geometry and ultrasonic transducer configuration. The calculation utilized an extension of an exact integral expression taken from reference 8 for calculating the normal acoustic particle displacement at the transmitted beam location on the sample surface. Note that the raw data image is partly obscured by vignetting on the left side of the image. The general agreement is good, but subtle phase variations predicted by the model are only partly visible in the raw data. Improvements in the signal to noise ratio will be needed to improve this correspondence between real and predicted data.

6. CONCLUSION

An optical imaging approach has been described for performing full-field imaging of acoustic wave motion at the surface of opaque materials. The method utilizes photorefractive dynamic holography and provides a displacement sensitivity of 0.1 nanometers using a Nd:YAG 532nm laser source. Acoustic images of the radiation scattered from buried simulated flaws deep within aluminum blocks was recorded at video frame rates. Acoustic reflection and wavefront characterization were compared favorably with directly calculated wavefront patterns using integral diffraction theory from a piston acoustic transducer. Acoustic wave images for scattering off of buried flat bottom holes were successfully recorded on the bottom sample surface, showing the transmitted radiation coupled with diffraction off the flat surface and sides of the hole. Successful imaging was also presented of the acoustic radiation reflected off the flat bottom of a hole onto the top sample surface, showing the reflected acoustic wavefronts and illustrating diffraction from the hole in the acoustic far-field. These results will be further verified with direct theoretical simulation using acoustic diffraction theory in future work. At present, the efficacy of the approach has been amply demonstrated providing a new noncontacting acoustic imaging methodology for acoustical imaging of buried flaws in materials.

ACKNOWLEDGEMENTS

This work was supported by the US Department of Energy under contract number DE-AC07-99ID13727.

REFERENCES

1. J.P. Monchalin and R. Héon, "Laser Ultrasonic Generation and Detection with a Confocal Fabry-Perot Interferometer," Materials Evaluation, 44, 1231 (1986).
2. C. B., SCRUBY and , L. E., DRAIN, *Laser Ultrasonics: Techniques and Application*s, (Adam Hildger, New York, 1990)
3. J. W. Wagner, *Physical Acoustics*, Vol.XIX, Eds. Thurston, R.N., and Pierce, A.D., (Academic Press, New York, 1990) Chp. 5.
4. K.L. Telschow, V. A. Deason, R. S. Schley and S. M. Watson, "Direct Imaging of Lamb Waves in Plates using Photorefractive Dynamic Holography," J.Acoust. Soc. Am. 106(5), 2578-2587 (1999).
5. Sorbothane, Inc., 2144 State Route 59 Kent, Ohio 44240
6. Ken L. Telschow, Vance A. Deason, David L. Cottle and John D. Larson III, "UHF Acoustic Microscopic Imaging of Resonator Motion" *Proceedings of the 2000 IEEE Ultrasonics Symposium*, October 22-25, San Juan, Puerto Rico, S.C. Schneider, M. Levy, B. R. McAvoy eds., IEEE, Piscataway, NJ. Vol.1, 631-634 (2000).
7. V. A. Deason, K.L. Telschow, R. S. Schley, S. M. Watson, "Imaging the Anisotropic Elastic Properties of Paper with the *INEEL Laser Ultrasonic Camera,*" CP509, *Reviews of Progress in Quantitative NDE*, edited by D. O. Thompson and D. E. Chimenti (2000 American Institute of Physics, 1-56396-930-0) 255-261.
8. Lester W. Schmerr Jr., Fundamentals of Ultrasonic Nondestructive Evaluation: A Modeling Approach, (Plenum Publishing, New York, 1998) chapter 8.